JAAS

Accepted Manuscript

This is an *Accepted Manuscript*, which has been through the Royal Society of Chemistry peer review process and has been accepted for publication.

Accepted Manuscripts are published online shortly after acceptance, before technical editing, formatting and proof reading. Using this free service, authors can make their results available to the community, in citable form, before we publish the edited article. We will replace this *Accepted Manuscript* with the edited and formatted *Advance Article* as soon as it is available.

You can find more information about *Accepted Manuscripts* in the Information for Authors.

Please note that technical editing may introduce minor changes to the text and/or graphics, which may alter content. The journal's standard Terms & Conditions and the Ethical guidelines still apply. In no event shall the Royal Society of Chemistry be held responsible for any errors or omissions in this *Accepted Manuscript* or any consequences arising from the use of any information it contains.

ROYAL SOCIETY OF CHEMISTRY

www.rsc.org/jaas

Chlorine isotope determination *via* the monitoring of the AlCl molecule by high-resolution continuum source graphite furnace molecular absorption spectrometry–a case study

F. V. Nakadi,[a,b] M.A.M.S. da Veiga,[a,b] M. Aramendía,[c] E. García-Ruiz[a] and M. Resano[a]*

[a]Department of Analytical Chemistry, Aragón Institute of Engineering Research (I3A), University of Zaragoza, Pedro Cerbuna 12, 50009, Zaragoza, Spain. E-mail: mresano@unizar.es

[b]While on leave from Departamento de Química, Faculdade de Filosofia, Ciências e Letras de Ribeirão Preto, Universidade de São Paulo, 14040-901, Ribeirão Preto-SP, Brazil

[c]Centro Universitario de la Defensa-Academia General Militar de Zaragoza, Carretera de Huesca s/n, 50090, Zaragoza, Spain

Abstract

This work investigates the possibility of obtaining isotopic information *via* the monitoring of the absorption spectra of a gaseous diatomic molecule generated in a graphite furnace and using a high-resolution (approx. 1.5 pm per pixel) monochromator (HR CS GFMAS). To test this concept, Cl was chosen as analyte and AlCl as the target species. The results demonstrate that, unlike what occurs with atomic spectra, under optimum conditions it is possible to acquire isotopic information by HR CS GFMAS in a straightforward way, as it is feasible to observe band heads for each Cl isotope (actually, for $Al^{35}Cl$ and $Al^{37}Cl$) that are separated, i.e., they act like two different molecules absorbing at different wavelengths.

The method proposed, based upon addition of both Pd and Al and the selection of peak height values, enables Cl isotopic analysis with precision values around 2% RSD for solutions with Cl contents at the mg L^{-1} level. Accurate values, within this uncertainty, can be directly obtained without requiring any method for mass bias correction. The potential of

isotope dilution for calibration is also explored, and it is proven how this approach can help in providing accurate results in situations where the occurrence of chemical interferences, a case frequently encountered for the HR CS GFMAS technique, hampers the use of other calibration approaches, as demonstrated for water analysis.

1. Introduction

Despite its toxicity, chlorine is a widely used industrial commodity. Cl is used in many different fields such as production of chlorinated solvents and other chemicals, water purification, plastics production and pulp and paper manufacture,[1] thus making it necessary to control the presence of this element at trace levels in a wide variety of samples.[2-9]

In addition to controlling the elemental content, investigating the isotopic composition of Cl can be of interest in different situations, as it may help, for instance, to track the source or the fate of different Cl species in the environment, or in biological fluids, or help in elucidating geochemical processes.[10] Some recent articles, based on the use of different techniques such as gas source mass spectrometry (often referred to as IR-MS[11]), thermal ionization mass spectrometry,[12,13] laser ablation multicollector-inductively coupled plasma mass spectrometry (MC-ICPMS),[14] ion chromatography MC-ICPMS,[15] gas chromatography-MS,[16] and high performance liquid chromatography-MS/MS,[17] have evaluated the isotope content of Cl in different matrices. These techniques rely on the high sensitivity and selectivity of mass spectrometry, which typically requires rigorous sample preparation to avoid matrix interferences.[18]

Some interesting alternatives to MS techniques, which may be worth exploring, are appearing in the literature recently. For instance, laser ablation molecular isotopic spectrometry (LAMIS), developed by Russo *et al*., explores the concept of wavelength isotopic shifts between diatomic molecules.[19,20] This technique can be seen as an evolution of LIBS, but instead of aiming at the monitoring of the emission spectra of elemental species, which are well-known to show very small isotopic variations, its goal is to evaluate and quantify isotopic shifts occurring for diatomic molecules, in which one of the atoms is the target analyte. These shifts are significantly larger than their atomic counterparts,[19] thus permitting to determine boron,[19,21,22] carbon,[19,23] hydrogen,[19,24] oxygen,[19] and strontium[25] isotopes, without requiring extensive sample preparation or a vacuum environment.

In principle, not only emission but also absorption could be used to obtain isotopic information. When the goal is to monitor atomic absorption, high-resolution continuum

source atomic absorption spectrometry (HR CS AAS) offers very significant advantages when compared to classic line source instrumentation,[26] such as improved possibilities to detect and correct for interferences and lower limits of detection.[27-32] In addition, this technique offers enough resolution (down to approx. 1 pm) to quantify different portions of an atomic line; however, even with such instrument, it is very challenging to detect the small energy variations occurring for different isotopes, owing to a number of well-known factors (i.e., collisional broadening, Doppler and Stark effects) that result in the broadening of the peaks.

So far, only one study has intended to attain isotopic information using HR CS AAS.[33] In such pioneering work, Wiltsche *et al.* used a flame as atomizer and tried to take advantage of the large mass difference existing between the two isotopes of B, ^{10}B and ^{11}B, to determine B ratios in steel samples. The authors found a less sensitive atomic line (around 208.9 nm) that shows a higher isotopic shift than the most sensitive one (249.8 nm): 208.95898 nm for ^{10}B and 208.95650 nm for ^{11}B. This difference is still too small to observe two fully resolved peaks with a HR CS FAAS instrument. However, it can still be appreciated that the B absorption profile shifts as a function of the boron isotopic ratio: the higher the % of ^{10}B, the higher the wavelength at which the peak maximum is found. Thus, it is in principle possible to determine the B isotopic composition. Nevertheless, since the isotopic shift of boron is very small, it is necessary to correct for possible instabilities of the monochromator in order to achieve sufficient precision and accuracy, which was done using a suitable internal standard (Fe or Ni) that was monitored in truly simultaneous mode. This approach was found satisfactory to distinguish different enrichment levels of ^{10}B (within 5%) in steel samples.

There is another advantage of HR CS instrumentation that should not be overlooked. That is the potential to monitor not only atomic but also complex and transient molecular spectra, as generated from a graphite furnace, which offers more sensitivity than a flame as atomizer. The resulting technique, high-resolution continuum source graphite furnace molecular atomic spectrometry (HR CS GFMAS) opens new ways to determine non-

metals,[34-36] for which it is hardly feasible to get access to their main atomic lines because they are located in the vacuum UV. But the use of HR CS GFMAS can also be beneficial for isotopic analysis, because, in the same way as explained before for LAMIS and emission spectrometry, the isotopic shifts found when monitoring molecular absorption spectra are expected to be much larger than those found for atomic absorption spectra.

This work aims at exploring this idea, the evaluation of the absorption of diatomic molecules, as a new possibility to acquire isotope data by means HR CS GFMAS. In order to investigate this new concept, which to the best of our knowledge has not been reported before in the literature, Cl has been selected as the analyte, owing to its relevance, as discussed before. Al has been chosen as the pair to create the AlCl molecule, which will be the target of the HR CS GFMAS monitoring, with the goal of producing isotopic transitions that could be spectrally resolved.

2. Experimental

2.1. Instrumentation

All the AlCl measurements were performed with a high-resolution continuum source atomic absorption spectrometer ContrAA 700, commercially available from Analytik Jena AG (Jena, Germany). The optical system comprises a xenon short-arc lamp (GLE, Berlin, Germany) operating in “hot-spot” mode as the radiation source, a high-resolution double echelle monochromator (DEMON) and a linear CCD array detector with 588 pixels, 200 of which are used for analytical purposes (monitoring of the analytical signal and BG correction), while the rest are used for internal functions, such as correcting for fluctuations in the lamp intensity. More details on this type of instrumentation can be found elsewhere.[26] This instrument is also equipped with a transversely heated graphite tube atomizer, pyrolytic graphite tubes, and both automated solid sampling and liquid sampling accessories. In this work, only liquids were introduced in the graphite furnace.

Moreover, an ICP mass spectrometer, NexION 300X (Perkin Elmer, USA) was used to validate the results obtained for the water samples by means of HR CS GFMAS.

2.2. Standards, reagents and samples

Two reference materials with a certified Cl isotopic composition (CRMs) were used in this work: SRM 975a Isotopic Standard for Chlorine (^{35}Cl atom percent: 75.774 ± 0.028%; ^{37}Cl atom percent: 24.226 ± 0.028%; absolute abundance ratio ^{35}Cl/^{37}Cl: 3.1279 ± 0.0047), available from the National Institute of Standards and Technology (NIST, USA), and ERM-AE642 Cl in water (^{37}Cl content: 4.375 ± 0.026 10^{-6} mol g^{-1}; absolute abundance ratio ^{35}Cl/^{37}Cl: 0.01914 ± 0.00048), available from the Institute for Reference Materials and Measurements (IRMM, Belgium). A stock standard Cl solution 1000 mg L^{-1} (Merck, Germany) was also used. In all of these materials, Cl was present as NaCl.

Other Cl solutions were prepared with diclofenac sodium (2-[(2,6-dichlorophenyl)amino]benzeneacetic acid sodium salt, Fluka, Switzerland), KCl, NH_4Cl and HCl (Merck). High-purity water (Trace Select Ultra, Cl level lower than 1 µg kg^{-1}, Fluka) was used for the preparation of all solutions. A stock standard Pd solution of 10 g L^{-1} (Merck) was diluted to 2 g L^{-1}, and this solution was applied as chemical modifier. A stock standard Al solution of 1000 mg L^{-1} (Merck) was also used to generate the AlCl molecule. A 10 g Ca L^{-1} solution was prepared by dissolving $CaCO_3$ (Merck) with 5% (v/v) HNO_3 (Merck), and used for an interference study. All the reagents were of analytical grade purity or higher.

Finally, two CRM samples with certified Cl levels were analyzed in this work: ION-915, natural water from Lake Superior (lot 1109), and KEJIM-02, soft water from Kejimkujik Lake (lot 0914), both available from Environment Canada (Canada). Five mineral water samples were acquired at local stores and analyzed as well.

2.3. Analysis of the samples

Samples were directly analyzed without any dilution step by means of HR CS GFMAS, using the instrumental parameters shown in **Table 1**. Both a calibration curve prepared with five Cl standards covering the interval 1-10 mg L^{-1} and isotope dilution (using a spike of 0.509 ^{35}Cl/^{37}Cl molar ratio and a Cl content of 1.09 mmol L^{-1}) were used for quantitation.

On the other hand, mineral water samples were also analyzed by means of ICPMS for validation purposes. The ICPMS parameters are shown in **Table 2**. In this case, samples were diluted using high-purity water and the calibration curve was constructed using five Cl

standards that covered the interval between 100 and 1000 μg L^{-1}. In all cases, three different sample aliquots were analyzed.

3. Results and discussion

3.1. Cl monitoring by HR CS GFMAS

3.1.1. Theoretical and experimental Cl isotopic monitoring

Contrary to what occurs with other non-metals such as F, P and S, the number of articles devoted to Cl monitoring by HR CS GFMAS is surprisingly low considering the importance of this element,[36] which probably indicates that its determination is not straightforward. So far, only three articles have reported on the use of this technique to determine Cl. The first two articles selected AlCl as the target molecule,[4,37] while the most recent one opted for SrCl.[9] In this work, we have selected AlCl, not only because it is a fairly sensitive and stable molecule (bond dissociation energy 511 kJ mol^{-1}), but also because Al is monoisotopic and, therefore, the potential isotopic shift should only obey to Cl variations. Furthermore, the isotopic shifts observed for this molecule are sufficiently large to be appreciated by means of HR CS GFMAS, as will be proved below.

The theoretical isotopic shift can be derived from the equation available in the classic book of Herzberg,[38] in a similar way as described by Russo *et al.*,[19] as shown below:

Eq. 1

$$\Delta v = (1-\rho)\left[\omega_e'\left(\mathrm{v}'+\frac{1}{2}\right)-\omega_e''\left(\mathrm{v}''+\frac{1}{2}\right)\right]-(1-\rho^2)\left[\omega_e'\mathrm{x}_e'\left(\mathrm{v}'+\frac{1}{2}\right)^2-\omega_e''\mathrm{x}_e''\left(\mathrm{v}''+\frac{1}{2}\right)^2\right]$$
$$+(1-\rho^3)\left[\omega_e'\mathrm{y}_e'\left(\mathrm{v}'+\frac{1}{2}\right)^3-\omega_e''\mathrm{y}_e''\left(\mathrm{v}''+\frac{1}{2}\right)^3\right]$$

where $\Delta\nu$ is the isotopic shift in cm^{-1}, v is the vibrational quantum number, ω_e is the harmonic frequency, $\omega_e x_e$ and $\omega_e y_e$ are the first and second anharmonic constants, respectively; $\rho=(\mu/\mu^i)^{1/2}$, where μ is the reduced mass of the molecule and i corresponds to the heavier isotope. The number of apostrophes denotes the electronic levels (two for the lower one, and one for the upper one) involved in the electronic transition.

The only difference with the equation used in ref. 19 is that we observed that, for the AlCl molecule and for the type of transitions investigated in our work (transitions between different vibrational levels), it is necessary to add a third term. In theory, the number of terms is infinite, but with these three terms shown above an excellent agreement between theoretical and experimental shifts can be obtained (R^2=0.99987).

Table 3 shows this comparison. The isotopic shift of the 261.418 nm transition could not be observed because the shift is too small for the resolution provided by the instrument (every pixel covers 1.47 pm in this wavelength region). For the rest of the transitions, the difference between the theoretical and experimental shifts was always lower than 2%.

It is important to stress that, unfortunately, the isotopic shift is inversely proportional to the sensitivity of the transition. This is probably due to the fact that the higher shifts occur for higher vibrational levels, which exhibit a lower population even at the relatively high temperature of a graphite furnace.

In order to better evaluate the potential of these transitions for isotopic analysis, a series of 2D spectra (Abs. *versus* wavelength) were acquired for a Cl solution with a 35/37 molar ratio close to unity (except for **Figure 1B**, as will be discussed below). These spectra are shown in **Figure 1**. As previously discussed, **Figure 1A** shows that for the 261.418 nm transition only a broad band can be detected, as the signals for the two isotopes are not resolved. This transition is the one typically selected for Cl elemental analysis.[4,37] The next transition in terms of sensitivity, 261.695 nm still did not show two different peaks, but it could be seen that the peak maximum shifts as a function of the isotopic composition. This aspect can be appreciated in **Figure 1B**, which compares the signal obtained for a spike enriched in ^{37}Cl with that occurring for another solution richer in ^{35}Cl. This is similar to the situation found by Wiltsche *et al.* when monitoring atomic lines for B isotopic analysis.[33] The next transition, 261.819 nm (**Figure 1C**), already shows two different peaks, the left one corresponding to Al^{37}Cl and the right one to Al^{35}Cl, although they are not well resolved. That would affect the ratio finally obtained, as the tailing of the Al^{37}Cl peak has a clear effect on the Al^{35}Cl signal, thus resulting in a 35/37 ratio that is biased high.

The 261.238 nm transition (**Figure 1D**) shows a better situation, as the peaks, while still not fully resolved, do not seem to overlap sufficiently to influence the ratio obtained in a significant way, since the ratio of both peaks is close to unity. This spectrum hints for the first time at the possibility of carrying out isotopic analysis by HR CS MAS with good resolution and in a straightforward manner, as the band head of each Cl isotope is separated, i.e., they act like two different molecules absorbing at different wavelengths. The situation for the next transitions (**Figure 1E** to **1H**) shows an even higher separation between the peaks, but at the cost of a decreasing signal. This can be problematic as the effect of the background structure may begin to affect the ratios obtained. Still, these transitions may be useful for higher Cl levels. For determinations at the mg L^{-1} level, the transition shown in **Figure 1D** was considered as the most suitable and was further used throughout the work.

3.1.2. Optimization of the working parameters

Once the most suitable wavelength was selected, other aspects were investigated. Two factors that can be critical for the formation of the AlCl molecule in the graphite furnace are (i) the amount of Al added, that should be enough to aim at the maximum Cl conversion into AlCl, and (ii) the amount of chemical modifier added, which may help in stabilizing both Al and, particularly, Cl species. Pd was chosen as chemical modifier and the amount of both Al and Pd were optimized, as shown in **Figure 2**.

Only a small AlCl absorbance variation was observed for Al contents greater than 5 µg (**Figure 2A**). Nonetheless, an amount of 10 µg was chosen for further studies to ensure the correct formation of the AlCl molecule. As for the Pd content (see **Figure 2B**), it is clear that it has a significant influence on the AlCl signal. Low Pd levels lead to poor sensitivity, while very high contents also provide a very low signal, probably because AlCl is no longer formed in significant amounts owing to the strong Pd competition. The optimum values range from 5 to 20 µg of Pd. A value of 20 µg was chosen for further studies.

The temperature program was subsequently optimized as well (see **Figure 3**). In the presence of Pd, a stable signal was obtained for a pyrolysis temperature of up to 500 ºC, with good agreement between the theoretical and experimental isotopic ratios. As for the

vaporization temperature, a plateau is reached for temperatures of 2100 ºC or higher. Use of 2200 ºC guarantees maximum sensitivity, a good peak definition while still preserving the lifetime of the graphite parts.

Finally, the AlCl signal obtained for five very different Cl species (diclofenac sodium, HCl, KCl, NH_4Cl and NaCl) under these optimum conditions was recorded. The temporal signals profiles obtained for $Al^{35}Cl$ are shown in **Figure 4**. As can be seen, no significant difference between them was observed (variations of both peak area and peak height were smaller than 6%). The same conclusion was reached for the $Al^{37}Cl$ transition. This confirms that the method developed shows potential for the monitoring of Cl isotopes regardless of the particular form in which Cl is found in the samples.

3.2. Quantification of the isotopic shift

3.2.1. Signal evaluation

Traditionally, in GFAAS it is preferable to integrate the absorbance peak along time, as it typically leads to better precision, and it may minimize the influence of the matrix on the final result. However, when the aim is to determine the isotopic composition, the situation could be different. Since there is no information on this issue, a study was performed evaluating the signals both in terms of peak area and of peak height, and also investigating the optimum number of detector pixels to be considered, which is another parameter that can significantly influence the final result.[39-41] **Figure 5A** shows the results obtained during this study for the main five AlCl transitions for which two separate $Al^{37}Cl$ and $Al^{35}Cl$ were detected, as discussed in section 3.1.1.

These results were obtained *via* analysis of a CRM (NIST 975a) with a certified Cl ratio that is shown in the figure (dotted line). As can be seen, the results for the first transition evaluated (around 261.82 nm) are biased high. This was expected because the two peaks for $Al^{37}Cl$ and $Al^{35}Cl$ are not well resolved in this case (see **Figure 1C**). However, the difference with the certified value is lower when peak height is selected. This difference increases with the number of detector pixels chosen for quantitation (which is logical,

because the degree of peak overlap is reduced when less pixels are selected). The precision obtained is also better for peak height.

The results obtained for the next transition (around 262.24 nm, spectrum shown in **Figure 1D**) are significantly better, and they are in good agreement with the reference value using both peak area and peak height. This is the transition that was initially selected as most promising, and these results confirmed its selection for Cl monitoring at the mg L^{-1} level.

The following transitions offer results than tend to be biased low. As discussed before, the problem of such transitions is that the sensitivity decreases with every one of them and the influence of the structured background on the ratio becomes more pronounced (see **Figures 1E** to **G**). This influence is more significant when peak area is selected instead of peak height, as could be anticipated. The precision, as shown by the error bars, is also significantly better when using peak height. Therefore, overall, use of peak height seems to be preferable for this type of analysis, and was adopted for further work. As for the number of pixels, it seems to be a critical aspect only if the $Al^{37}Cl$ and $Al^{35}Cl$ are closely located. As a general rule, a number of 3 pixels was selected (central pixel ± 1), but this is a parameter that should be evaluated also depending on the analyte content for every particular situation, as higher contents may lead to peak broadening and a higher chance of spectral overlap.

The precision that can be achieved under these optimum conditions was evaluated by isotope analysis of a solution of NIST 975a with a concentration of 20 mg L^{-1}. The results obtained after 20 replicates are shown in **Figure 5B**. As can be seen, the typical variation observed for a particular individual isotopic AlCl transition is rather high (approx. 8%), but when isotope ratios are calculated a much better value is obtained, as all the correlated sources of noise are compensated. In this way, a 2% RSD value can be considered as typical for Cl isotopic analysis under these conditions. This value is clearly insufficient if the goal is to monitor natural isotopic variations, which for Cl are expected to be much lower, but it may be enough for performing tracer experiments or to use isotope dilution for calibration, thus opening new possibilities for the HR CS GFMAS technique. Furthermore, it can be

stressed that, unlike what occurs with most MS techniques, in which at least correction for the instrumental mass bias is required, the results demonstrate than an accurate ratio, within the uncertainty mentioned above, can be directly obtained without performing any type of correction.

3.2.2. Correction for spectral overlap in the case of high 37/35 ratios

Despite the satisfactory results obtained so far for solutions showing a $^{35}Cl/^{37}Cl$ molar ratio close to the natural one, when performing tracer experiments or using isotope dilution, ratios that differ from the natural one are often used. That could represent a potential problem, because the tailing of the $Al^{37}Cl$ may influence the $Al^{35}Cl$ signal (see **Figure 1**) in cases when spikes with a high 37/35 ratio are used. Thus, in order to check the robustness of the method developed, solutions with very different ratios were prepared by mixing different amounts of two reference materials (NIST 975a and ERM-AE642), and their isotope ratio was calculated experimentally by HR CS GFMAS using the optimum parameters discussed before and summarized in **Table 1**.The results obtained are shown in **Figure 6A**. As can be seen, a very good agreement between theoretical and experimental values was obtained for 37/35 ratios up to 1.5. However, spikes showing a higher 37/35 ratio tend to provide results that are biased low, which indicates a potential overlap, as discussed above.

This problem could be solved using signal deconvolution. However, most deconvolution approaches are not really suitable for this particular situation, because they are based on Gaussian or Lorentzian functions, which assume symmetric peak profiles. That is clearly not the case in this work, as the peaks show a longer right tail (see **Figure 1**). Thus, a different model was evaluated to circumvent this problem, following the steps shown in **Figure 7**. **Figure 7A** shows the initial peak profile, which shows a potential overlap of the $Al^{37}Cl$ tail on the $Al^{35}Cl$ signal. **Figure 7B** shows the same data in more detail, focusing in the range between pixel 91 and pixel 150, and also showing the individual detector pixels recorded. After examining this area, those values that could be affected by the presence of the $Al^{35}Cl$ molecule are removed, and the rest of the data is fitted using an asymptotic

regression model (**Figure 7C**). Then, finally, the contribution of the $Al^{37}Cl$ signal can be subtracted.

Figure 6B shows the results obtained when this correction is applied to those values with a 37/35 ratio higher than 1.5. As can be seen, a good agreement between theoretical and experimental data is now obtained for the entire interval investigated. Therefore, this model can be considered as suitable for spectral overlap correction.

3.3. Ca interference

One of the main differences between HR CS GFMAS and HR CS GFAAS is that the former is more prone to suffer from chemical interferences, because the presence of other elements in the matrix may result in the formation of a molecule different from the target one at some point of the pyrolysis and/or vaporization steps. This fact can affect the absorbance finally obtained and make it difficult to develop a straightforward calibration procedure. Therefore, it is important to choose a target molecule that is stable even at high temperatures, such as it is the case of AlCl (bond dissociation energy 511 kJ mol^{-1}), to minimize this effect. However, that is not the only issue to consider, because the concentration of the competing species may also play a role. One element that is usually present at high levels in many types of samples and can interact with Cl is Ca (CaCl bond dissociation energy 409 kJ mol^{-1}). Thus, this potential issue was investigated in more detail for varying amounts of Ca.

Figure 8A shows that, indeed, the presence of a high amount of Ca may represent a problem. As can be seen, for low levels of Ca the signal of Al is hardly affected. Hovewer, for Ca/Cl molar ratios higher than 2, the AlCl signal tends to rise. Even though ultimately the AlCl molecule is formed (which is logical because it is more stable and there is more Al available -10 µg- than Ca), Ca seems to act like a chemical modifier,[42] helping in forming AlCl with more efficiency. However, for Ca/Cl ratios higher than 90 the signal for AlCl begins to decrease, until it reaches a point where AlCl is practically not formed owing to the higher availability of Ca atoms.

While it could be interesting to further investigate on the vaporization mechanism of AlCl in the presence of Ca and Pd, such aspect is out of the scope of the present work. What is relevant here is to stress that the presence of a high but unknown amount of Ca in the sample will make it very difficult to obtain accurate results when constructing the calibration curve with aqueous standards, as this element will have a clear impact on the AlCl absorbance finally obtained.

Isotope analysis brings a new possibility to circumvent this kind of problem, which so far has been limited to MS techniques. Instead of using the cumbersome standard addition method, or matrix-matched standards, the use of isotope dilution (ID) can help in successfully overcoming this type of interference. In fact, **Figure 8B** shows that, despite the high fluctuations observed for the individual AlCl signal for varying amounts of Ca, the value obtained for the $Al^{35}Cl/Al^{37}Cl$ ratio remains very stable, which clearly indicates that ID may provide satisfactory results in this case.

3.4. Cl determination in water using ID for calibration

To explore the robustness of an ID method in comparison with a conventional calibration strategy, two different natural water CRMs (ION-915 and KEJIM-02) were selected for analysis. For the latter approach, a calibration curve was prepared with 5 points ranging from 1 to 10 mg L^{-1}. The calibration curve showed a R^2 coefficient of 0.9998, a limit of detection (LOD) of 0.30 mg L^{-1} and a limit of quantification (LOQ) of 1.0 mg L^{-1}. The results obtained for the samples are shown in **Table 4**. As can be seen, a result that is in good agreement with the Cl certified value was obtained for KEJIM-02, but the same was not true for the other sample, ION-915, for which a result biased high was found. This fact could be explained considering the Ca/Cl content of the samples, which is much higher in the case of ION-915 (13.7 mg L^{-1} Ca) than of KEJIM-02 (0.852 mg L^{-1} Ca), thus likely influencing the absolute AlCl absorbance signal, as demonstrated in the previous section.

Alternatively, the same samples were also analyzed using the conditions shown in **Table 1** and ID for calibration, as described in section 2.3. The calculations for the ID technique and for estimation of the LOD are discussed elsewhere.[43] The LOD was estimated

to be of 0.25 mg L^{-1}. As also shown in **Table 4**, the concentrations found by means of ID for both samples were in good agreement with the certified values, proving that this calibration technique can circumvent the interference detected in a simple way.

To further test the robustness of the ID approach, five commercial mineral water samples covering a wide range of Cl levels were also subjected to analysis. The results obtained are shown in **Table 5**. As can be seen, an excellent agreement with the expected values (as indicated by the producer in the label) was always attained. No different could be drawn by means of the t-Student test (95% confidence interval). The results obtained by means of ICPMS are also provided as a means of further result validation.

4. Conclusion

This work explores for the first time the potential of HR CS GFMAS for isotope analysis, focusing on Cl monitoring after formation of the AlCl molecule. The results obtained confirm that, by monitoring molecular instead of atomic spectra, it is possible to observe an isotopic shift that is large enough to appreciate two different peaks, each one corresponding to an isotope, which are sufficiently resolved to allow their quantification, regardless of the chemical form in which Cl is present in the sample.

The method developed, based on addition of Pd and Al, and the monitoring of peak height values, enables the isotopic analysis of Cl at the mg L^{-1} level with precision values around 2% RSD, not requiring any method for mass bias correction. However, if a spike with a high 37/35 ratio is to be monitored and a spectral overlap is detected, it is necessary to perform a deconvolution to correct for this interference.

Furthermore, it was demonstrated that using ID for calibration is feasible in this context and provides a novel -so far only used by MS techniques- and very powerful strategy to determine Cl in samples in which otherwise chemical interferences are detected, as demonstrated for water analysis.

Acknowledgements

This work has been funded by the Spanish Ministry of Economy and Competitiveness (project CTQ2012-33494) and the Aragón Government (Fondo Social Europeo). The authors are also grateful to Capes/PDSE for the mobility grant under process BEX 4250/14-1.

References

1. R.B. Evans, *Lung*, 2004, **183**, 151–167.
2. M.D. Huang, H. Becker-Ross, S. Florek, U. Heitmann and M. Okruss, *Spectrochim. Acta Part B*, 2006, **61**, 959–964.
3. A. Doyle, A. Saavedra, M.L.B. Tristão, L.A.N. Mendes and R.Q. Aucélio, *Spectrochim. Acta Part B,* 2013, **86**, 102–107.
4. M. Fechetia, A.L. Tognon and M.A.M.S. da Veiga, *Spectrochim. Acta Part B,* 2012, **71-72**, 98–101.
5. J.S. de Gois, É.R. Pereira, B. Welz and D.L.G. Borges, *Spectrochim. Acta Part B,* 2015, **105**, 12–17.
6. M.U. Rahim, X. Gao, and H. Wu, *Fuel*, 2014, **129**, 314–317.
7. T.A. Labutin, A.M. Popov, S.M. Zaytsev, N.B. Zorov, M.V. Belkov, V.V. Kiris and S.N. Raikov, *Spectrochim. Acta Part B,* 2014, **99**, 94–100.
8. P.A. Mello, J.S. Barin, F.A. Duarte, C.A. Bizzi, L.O. Diehl, E.I. Muller and E.M.M. Flores, *Anal. Bioanal. Chem.*, 2013, **405**, 7615–7642.
9. É.R. Pereira, B. Welz, A.H.D. Lopez, J.S. de Gois, G.F. Caramori, D.L.G. Borges, E. Carasek and J.B. de Andrade, *Spectrochim. Acta Part B,* 2014, **102**, 1–6.
10. M. Baskaran, Ed., *Handbook of Environmental Isotope Geochemistry*, Springer-Verlag, Berlin-Heidelberg, 2012.
11. N.C. Sturchio, J.K. Böhlke, A.D. Beloso Jr., S.H. Streger, L.J. Heraty and P.B. Hatzinger, *Environ. Sci. Technol.*, 2007, **41**, 2796–2802.
12. A. Sun, Q. Xu, S. Xu, H. Shen, J. Sun and Y. Zhang, *Chem. Geol.*, 2014, **381**, 21–25.
13. C. Luo, Y. Xiao, H. Wen, H. Ma, Y. Ma, Y. Zhang, Y. Zhang and M. He, *Appl. Geochem.*, 2014, **47**, 141–149.
14. J. Fietzke, M. Frische, T.H. Hansteen and A. Eisenhauer, *J. Anal. At. Spectrom.*, 2008, **23**, 769–772.
15. Y. Zakon, L. Halicz and F. Gelman, *Anal. Chem.*, 2014, **86**, 6495–6500.
16. C. Wiegert, M. Mandalakis, T. Knowles, P.N. Polymenakou, C. Aeppli, J. Macháčková, H. Holmstrand, R.P. Evershed, R.D. Pancost and Ö. Gustafsson, *Environ. Sci. Technol.*, 2013, **47**, 6449–6456.
17. M. Wu, Y. Qian, J.M. Boyd, S.E. Hrudey, X.C. Le and X.-F. Li, *J. Chromatogr. A*, 2014, **1359**, 156–161.
18. F. Vanhaecke and P. Degryse, Eds., *Isotopic Analysis: Fundamentals and Applications using ICP-MS*, Wiley-VCH, Weinheim, 2012.
19. R.E. Russo, A.A. Bol'shakov, X. Mao, C.P. McKay, D.L. Perry and O. Sorkhabi, *Spectrochim. Acta Part B,* 2011, **66**, 99–104.
20. R.E. Russo, X. Mao, J.J. Gonzalez, V. Zorba and J. Yoo, *Anal. Chem.*, 2013, **85**, 6162–6177.
21. X. Mao, A.A. Bol'shakov, D.L. Perry, O. Sorkhabi and R.E. Russo, *Spectrochim. Acta Part B,* 2011, **66**, 604–609.
22. A. Sarkar, X. Mao and R.E. Russo, *Spectrochim. Acta Part B,* 2014, **92**, 42–50.
23. M. Dong, X. Mao, J.J. Gonzalez, J. Lu and R.E. Russo, *Anal. Chem.*, 2013, **85**, 2899–2906.
24. A. Sarkar, X. Mao, G.C.Y. Chan and R.E. Russo, *Spectrochim. Acta Part B,* 2013, **88**, 46–53.
25. X. Mao, A.A. Bol'shakov, I. Choi, C.P. McKay, D.L. Perry, O. Sorkhabi and R.E. Russo, *Spectrochim. Acta Part B,* 2011, **66**, 767–775.
26. B. Welz, H. Becker-Ross, S. Florek and U. Heitmann, *High-Resolution Continuum*

Source AAS. The Better Way to do Atomic Absorption Spectrometry, Wiley-VCH, Weinheim, 2005.

27. M. Resano, F. Vanhaecke and M.T.C. de Loos-Vollebregt, *J. Anal. At. Spectrom.*, 2008, **23**, 1450-1475.
28. B. Welz, S. Morés, E. Carasek, M.G.R. Vale, M. Okruss and H. Becker-Ross, *Appl. Spectrosc. Rev.*, 2010, **45**, 327–354.
29. M. Resano and E. García-Ruiz, *Anal. Bioanal. Chem.,* 2011, **399**, 323–330.
30. M. Resano, M.R. Flórez and E. García-Ruiz, *Spectrochim. Acta Part B,* 2013, **88**, 85–97.
31. B. Welz, M.G.R. Vale, É.R. Pereira, I.N.B. Castilho and M.B. Dessuy, *J. Braz. Chem. Soc.*, 2014, **25**, 799–821.
32. M. Resano, M. Aramendía and M.A. Belarra, *J. Anal. At. Spectrom.,* 2014, **29**, 2229–2250.
33. H. Wiltsche, K. Prattes, M. Zischka and G. Knapp, *Spectrochim. Acta Part B,* 2009, **64**, 341–346.
34. B. Welz, F.G. Lepri, R.G.O. Araujo, S.L.C. Ferreira, M.D. Huang, M. Okruss and H. Becker-Ross, 2009, **647**, 137–148.
35. D.J. Butcher, *Anal. Chim. Acta*, 2013, **804**, 1–15.
36. M. Resano, M.R. Flórez and E. García-Ruiz, *Anal. Bioanal. Chem.,* 2014, **406**, 2239–2259.
37. U. Heitmann, H. Becker-Ross, S. Florek, M.D. Huang and M. Okruss, 2006, **21**, 1314–1320.
38. G. Herzberg, *Molecular Spectra and Molecule Structure. I. Spectra of Diatomic Molecules*, D. Van Nostrand, 2nd edn., New York, 1950.
39. U. Heitmann, B. Welz, D.L.G. Borges and F.G. Lepri, *Spectrochim. Acta Part B,* 2007, **62**, 1222–1230.
40. M. Resano, J. Briceño and M.A. Belarra, *Spectrochim. Acta Part B,* 2009, **64**, 520–529.
41. J. Briceño, M.A. Belarra, K.A.C. de Schamphelaere, S. Vanblaere, C.R. Janssen, F. Vanhaecke and M. Resano, *J. Anal. At. Spectrom.*, 2010, **25**, 503–510.
42. R. Nowka, K. Eichardt and B. Welz, *Spectrochim. Acta Part B,* 2000, **55**, 517–524.
43. M. Resano, M. Aramendía and F. Vanhaecke, *J. Anal. At. Spectrom.,* 2006, **21**, 1036–1044.
44. R.W.B. Pearse and A.G. Gaydon, *The identification of molecular spectra*, Chapman & Hall, 3rd edn., London, 1963.

Table 1. Instrumental parameters used to determine Cl by monitoring the AlCl molecule using HR CS GFMAS.

Electronic transition	$X^1\Sigma^+ \rightarrow A^1\Pi$
Wavelengths	262.238 nm ($Al^{35}Cl$)
	262.222 nm ($Al^{37}Cl$)
Number of detector pixels summed per line	3 (4.65 pm)
Reactant / Chemical modifier	Al (10 µg) / Pd (20 µg)
Sample volume	10 µL

Temperature program

Step	Temperature / ºC	Ramp / ºC s^{-1}	Hold / s	Ar gas flow / L min^{-1}
Drying	90	3	20	2.0
Drying	110	5	20	2.0
Pyrolysis	500	300	25	2.0
Vaporization	2200	1500	5	0
Cleaning	2500	500	4	2.0

Table 2. Instrumental parameters used to determine Cl by means of ICPMS.

RF power / W	1600
Plasma gas flow rate (Ar) / L min^{-1}	18
Nebulizer gas flow rate (Ar) / L min^{-1}	1.0
Auxiliary gas flow rate (Ar) / L min^{-1}	1.2
Scan mode	Peak hopping
RPq	0.25
Dwell time / ms	150
Sweeps / Reading	1
Readings / Replicate	20
Number of replicates	10
Nuclides monitored	$^{35}Cl^{+}$

Table 3. Experimental and theoretical isotopic shifts found for the analytical band heads of the AlCl molecule ($X^1\Sigma^+ \rightarrow A^1\Pi$ electronic transition) by HR CS GFMAS for different vibrational transitions (v', v"). The isotopic shift was calculated using equation 1 and converted to wavelength for correlation with experimental data. The relative sensitivity was compared with the most sensitive line (261.418 nm) and, when two separate peaks were observed, the $Al^{35}Cl$ and $Al^{37}Cl$ signals were summed.

λ/nm*	**λ_{exp} / nm**	**v',v"**	**$\Delta\lambda_{calc}$ / pm**	**$\Delta\lambda_{exp}$ / pm**	**Relative sensitivity / %**
261.44	261.418	0,0	1.37	---	100
261.70	261.695	1,1	4.86	4.8	62
261.82	261.819	2,2	9.61	9.6	30
262.24	262.238	3,3	16.0	15.6	26
262.70	262.697	4,4	24.2	24.3	16
263.22	263.216	5,5	34.8	35.3	7.4
263.81	263.807	6,6	48.0	48.1	3.2
264.49	264.490	7,7	64.3	64.5	1.1

*Data obtained from reference 44.

Table 4. Determination of Cl by HR CS GFMAS when constructing the curve with Cl aqueous standard solutions or by means of isotope dilution (ID). Experimental uncertainties are expressed as 95% confidence intervals (n = 3).

Sample	Cl concentration / mg L^{-1}		
	Certified	HR CS GFMAS	ID-HR CS GFMAS
ION-915	1.42 ± 0.02	2.04 ± 0.15	1.49 ± 0.08
KEJIM-02	5.79 ± 0.41	5.72 ± 0.77	5.78 ± 0.07

Table 5. Cl determination by means of HR CS GFMAS (using ID for calibration) and of ICPMS in five different commercial mineral water samples. Uncertainties are expressed as 95% confidence intervals (n = 3).

Sample	Cl concentration / mg L^{-1}		
	Label	ID-HR CS GFMAS	ICPMS
Veri	1.9	1.99 ± 0.15	1.87 ± 0.07
Fonter	5.1	5.27 ± 0.35	5.06 ± 0.38
Solán de Cabras	7.4	7.33 ± 0.30	7.17 ± 0.30
Aquarel Abetos	8.5	8.52 ± 0.17	8.08 ± 0.52
Fontecabras	49.5	49.9 ± 2.5	54.5 ± 2.8

Figure captions

Figure 1. Spectra of AlCl (1:1 $^{35}Cl/^{37}Cl$ molar ratio solution) at wavelengths of: (A) 261.418 nm; (B) 261.695 nm; (C) 261.819 nm; (D) 262.238 nm; (E) 262.697 nm; (F) 263.216 nm; (G) 263.807 nm; and (H) 264.490 nm. They were obtained for 400 ng Cl, 10 µg Al and 20 µg Pd. However, Figure 1B shows two different spectra: in black, the one obtained for 400 ng Cl of CRM NIST 975a (^{35}Cl 75.774%), and in red the one obtained for 400 ng Cl of CRM AE642 (^{37}Cl 98.122%).

Figure 2. Optimization of the (A) Al and (B) Pd amount used to monitor $Al^{35}Cl$ by HR CS GFMAS for 200 ng of Cl at the 262.238 nm line. 20 µg of Pd were added during the Al optimization, and 10 µg of Al were added during the Pd optimization. The three central pixels were summed for quantitation. Error bars represent the standard deviation (n = 5).

Figure 3. Optimization of the pyrolysis and vaporization temperatures to monitor AlCl by HR CS GFMAS for 200 ng of Cl (1.08 $^{37}Cl/^{35}Cl$ molar ratio) at the 262.222 ($Al^{37}Cl$) and 262.238 ($Al^{35}Cl$) nm transitions when adding 10 µg Al and 20 µg Pd. A pyrolysis temperature of 300 ºC was set for the vaporization study, and a vaporization temperature of 2400 ºC for the pyrolysis study. The three central pixels of each transition were summed for quantitation. Error bars represent the standard deviation (n = 5).

Figure 4. Comparison of the temporal peak profiles obtained for five different Cl species (250 ng Cl) when monitoring the 262.238 nm $Al^{35}Cl$ transition. The three central detector pixels were summed to represent the profile.

Figure 5. A) Evaluation of the accuracy and precision obtained for the quantification of the Cl ratio for a solution (200 ng Cl) of CRM NIST 975a (35/37=3.1279 ± 0.0047) for different AlCl transitions as a function of the way in which the signal is processed

and quantified. Values in blue were obtained using peak area, and values in green using peak height, while a lighter color intensity indicates a higher number of detector pixels (1, 3, 5 or 7) selected in both cases. In the case of using peak height, the absorbance recorded by those detector pixels at the time at which the maximum peak height appears was summed. Error bars represent the standard deviation (n = 5). B) Comparison of the variations observed for a series of 20 replicates for a solution (200 ng Cl) of CRM NIST 975a when monitoring the individual 262.222 ($Al^{37}Cl$) and 262.238 ($Al^{35}Cl$) nm transitions (left y-axis) or when calculating the Cl ratio from the same set of data (right y-axis). The red dashed line represents the certified value. The blue line and the blue interval surrounding it represent the average value of the 20 replicates and its uncertainty (as standard deviation), respectively.

Figure 6. Correlation between the experimental (as obtained *via* HR CS GFMAS) and theoretical (as prepared by properly mixing two certified reference materials) $^{37}Cl/^{35}Cl$ ratio when monitoring the 262.222 nm ($Al^{37}Cl$) and 262.238 nm ($Al^{35}Cl$) transitions for solutions containing 200 ng Cl. (A) without any mathematical deconvolution and (B) after mathematical deconvolution, as shown in Figure 7. Error bars represent the standard deviation (n = 5).

Figure 7. Spectral overlap correction performed at 262.238 nm for a Cl (500 ng) spike with a $^{37}Cl/^{35}Cl$ molar ratio = 2.5. (A) raw spectrum obtained at the time that provides the peak maximum; (B) effect of the $Al^{37}Cl$ signal tail on the $Al^{35}Cl$ peak; (C) application of asymptotic regression model ($y = a - bc^x$) using Origin 9.1 software; (D) estimation of the actual $Al^{35}Cl$ peak.

Figure 8. Study of the Ca interference. (A) $Al^{35}Cl$ absorbance signal, as recorded at 262.238 nm, and (B) $Al^{35}Cl/Al^{37}Cl$ absorbance ratio as a function of the Ca content,

for solutions containing 100 ng Cl, 10 µg Al and 20 µg Pd. Error bars represent 2 s (n = 5).

Figure 1

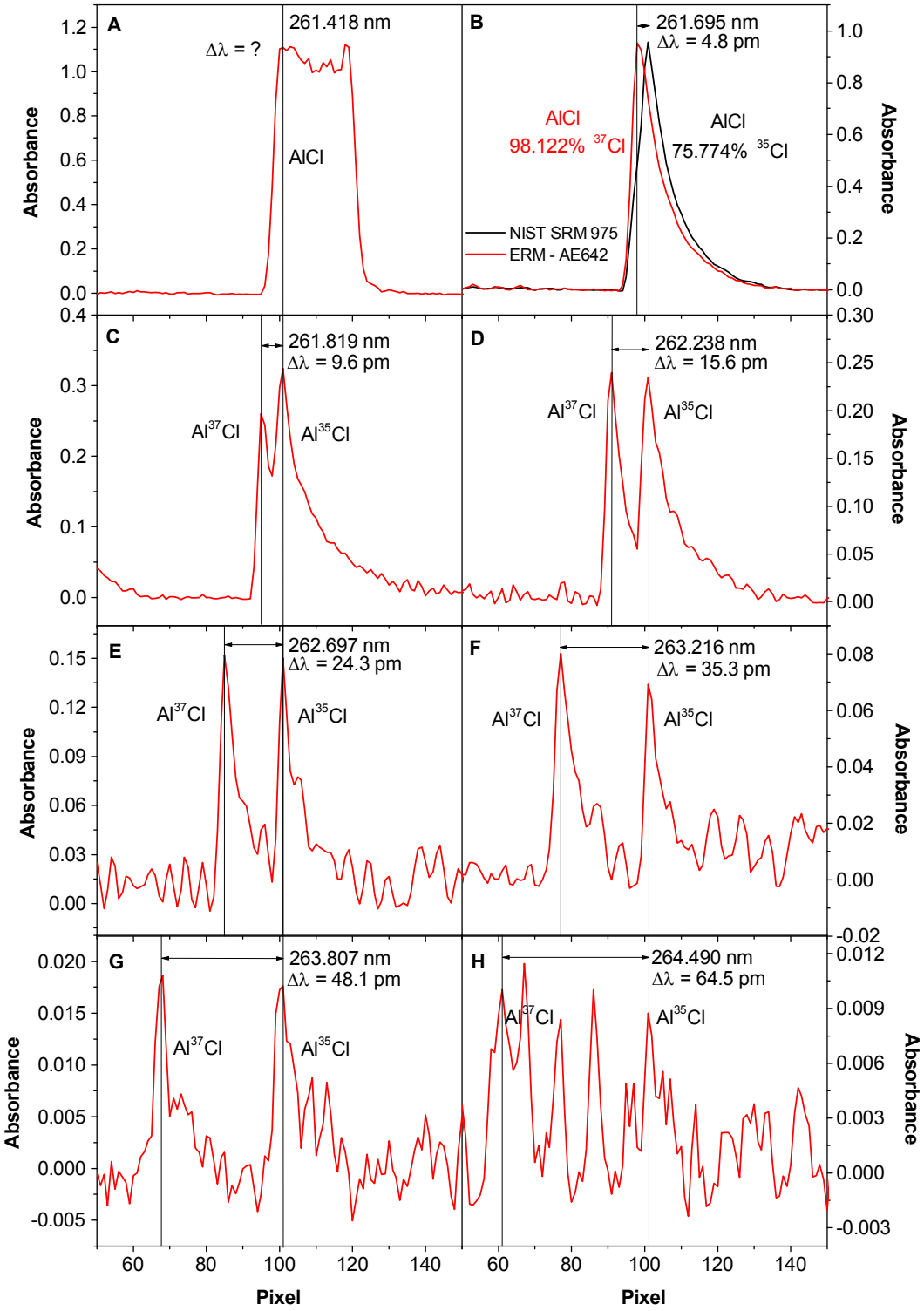

Figure 2

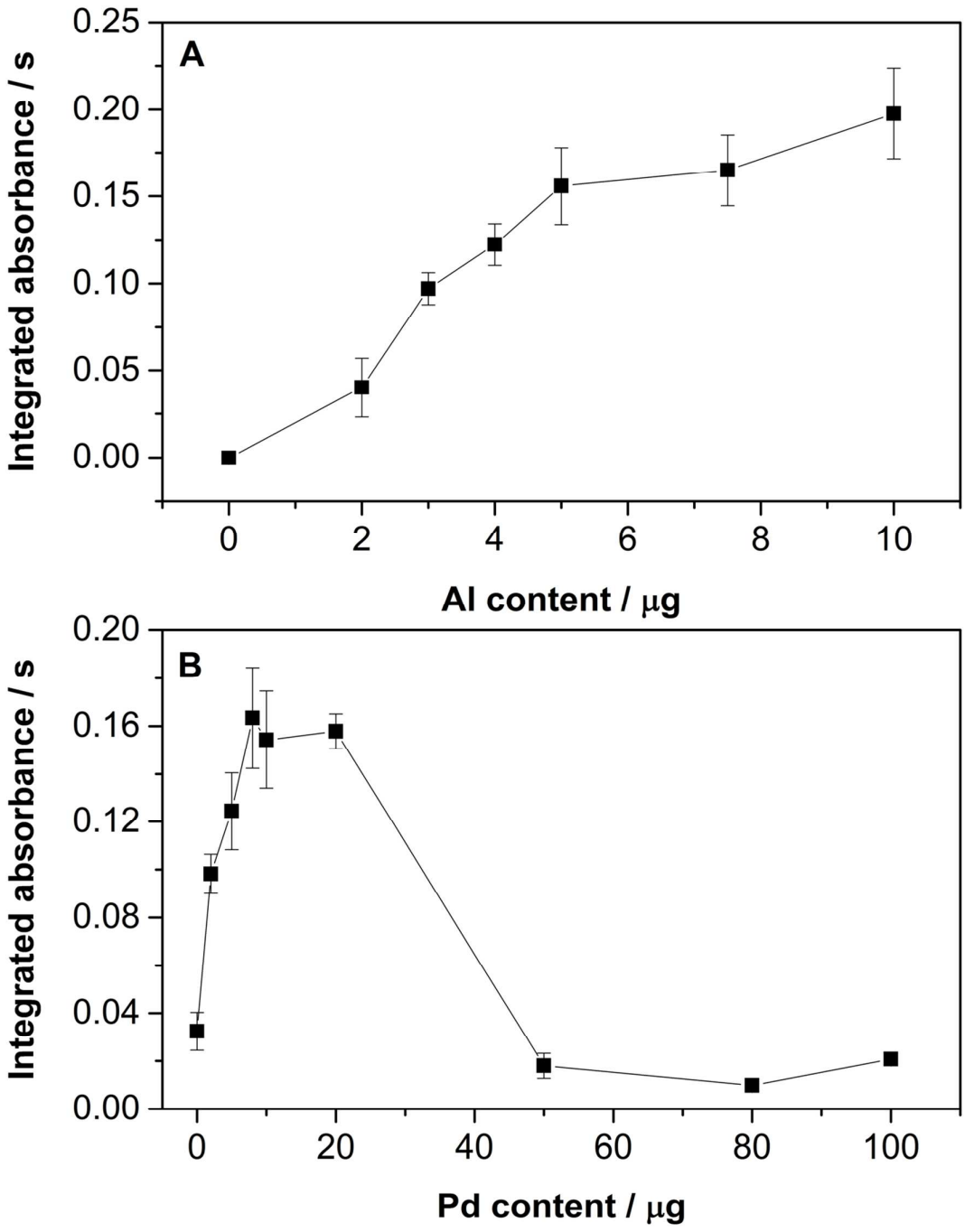

Figure 3

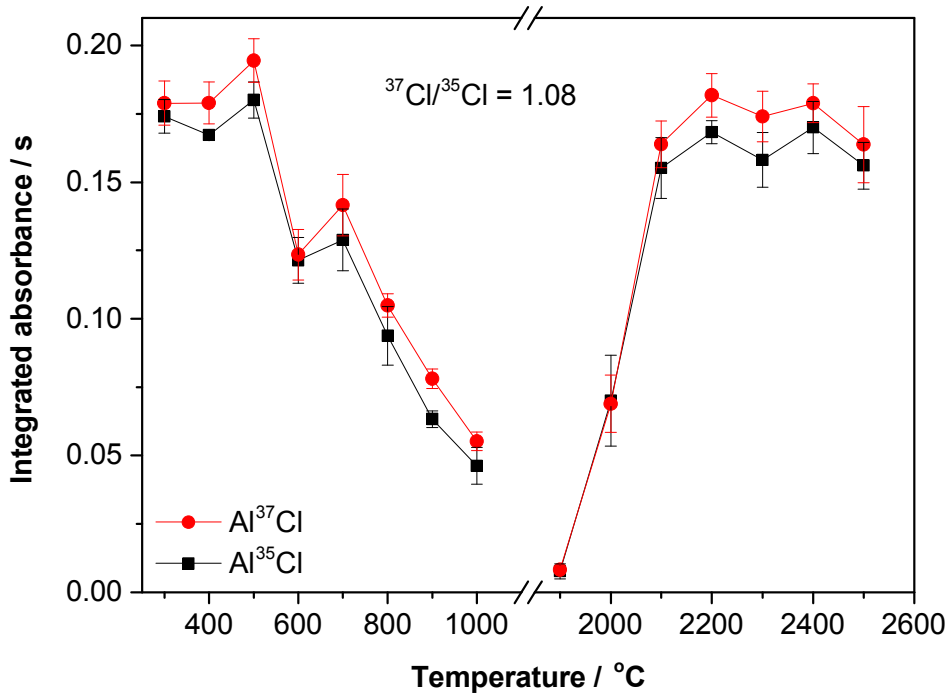

Figure 4

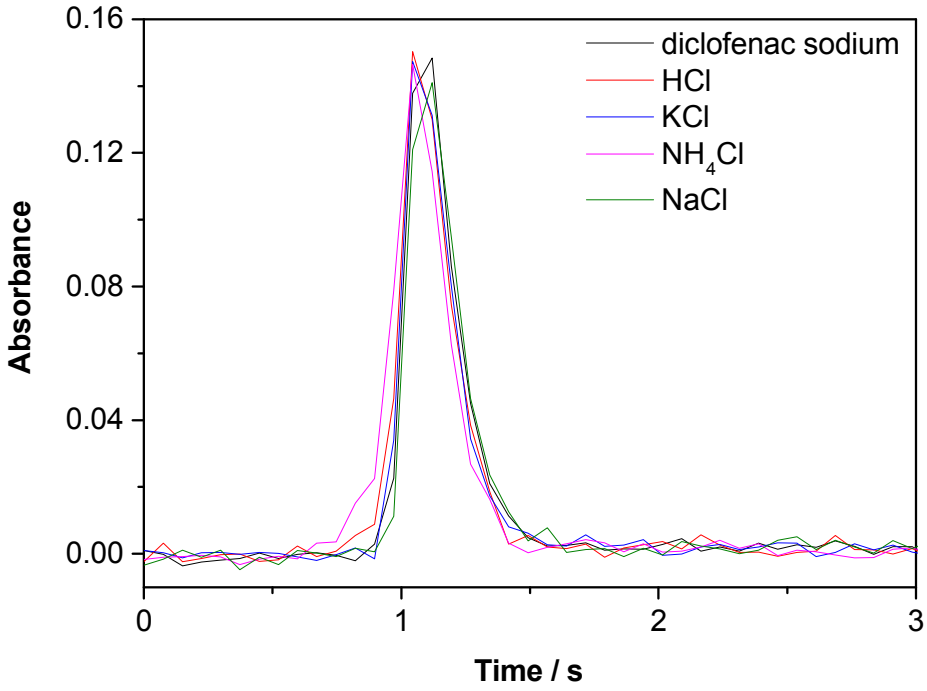

Figure 5

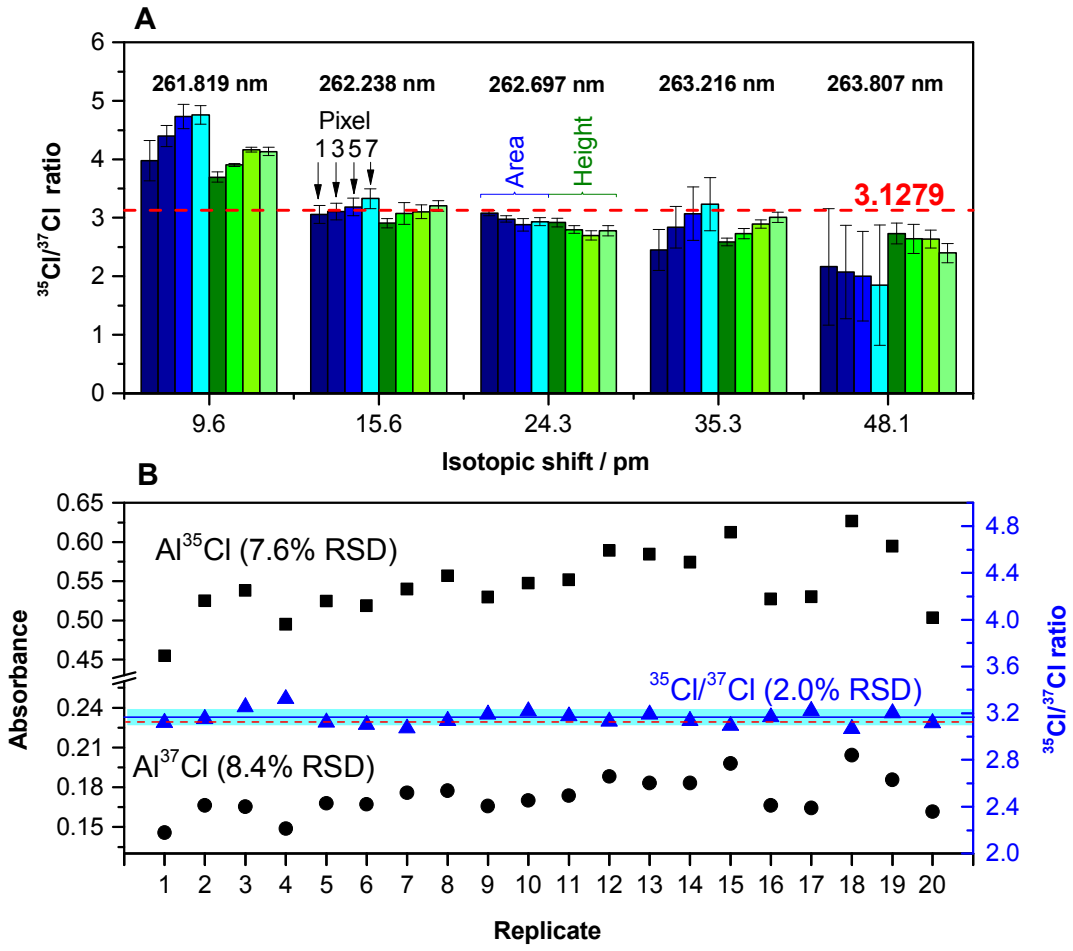

Figure 6

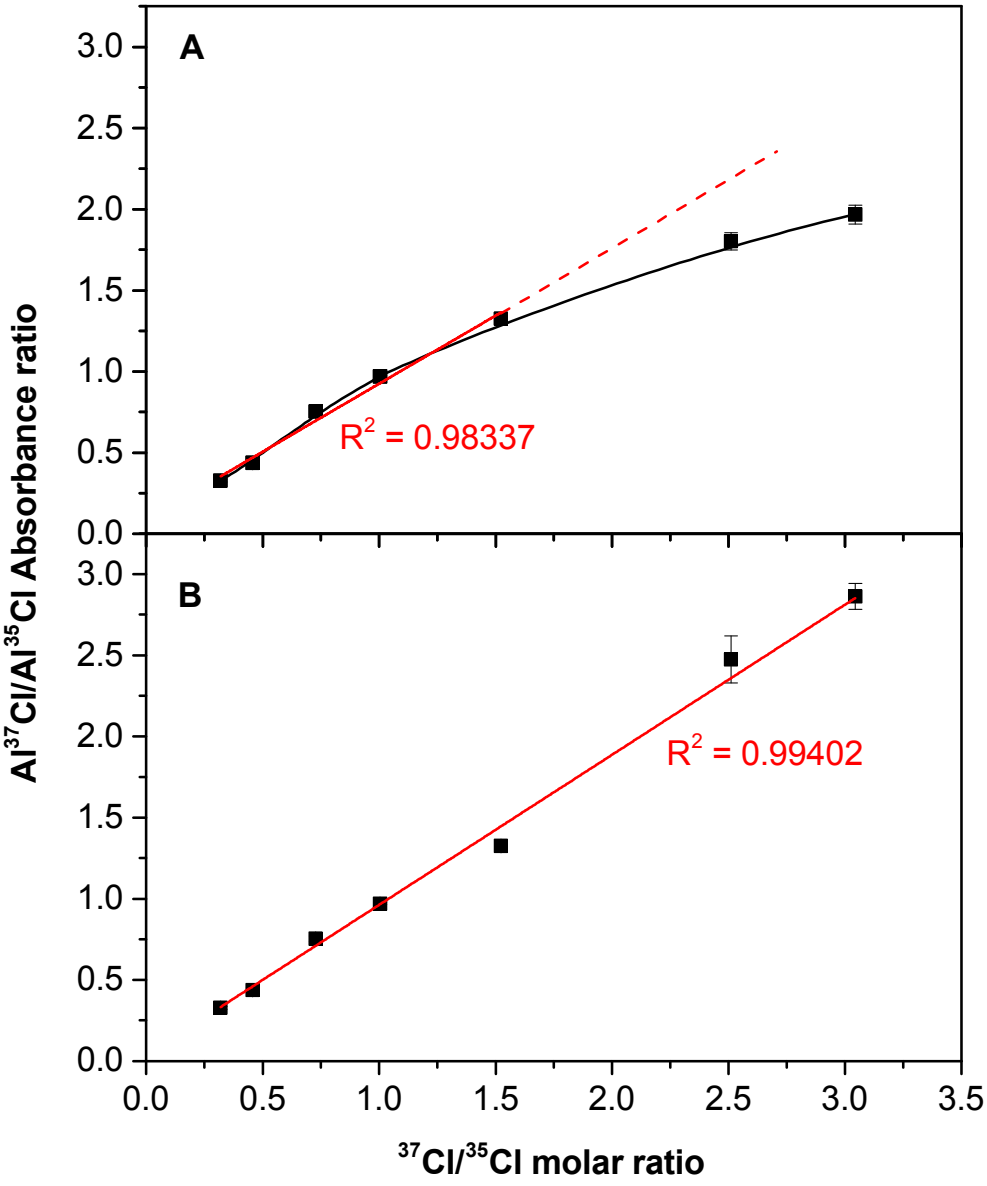

Figure 7

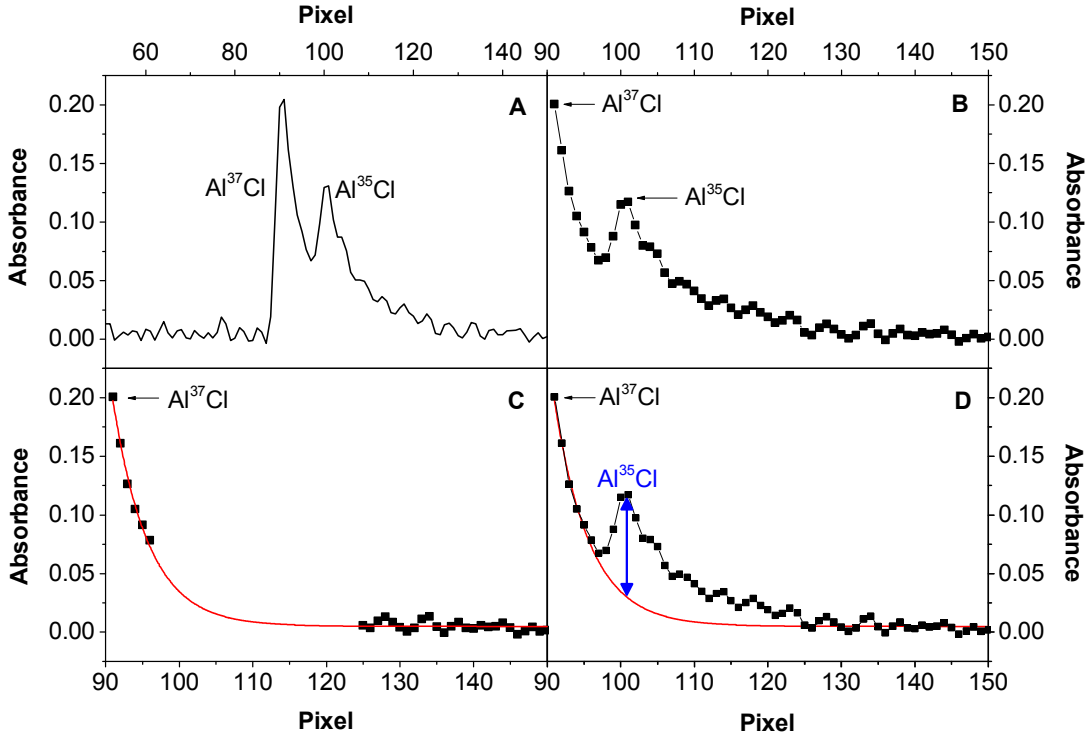

Figure 8

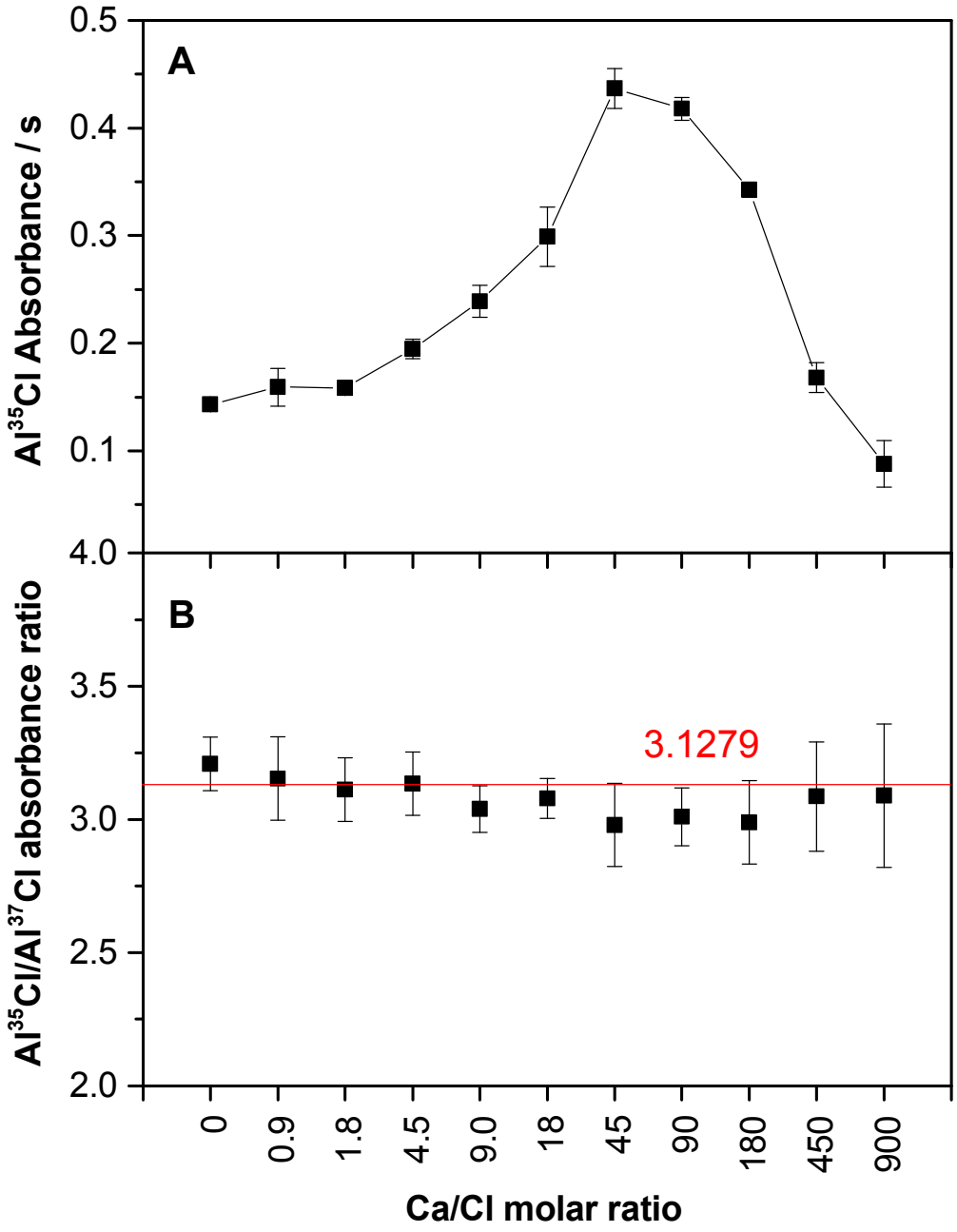

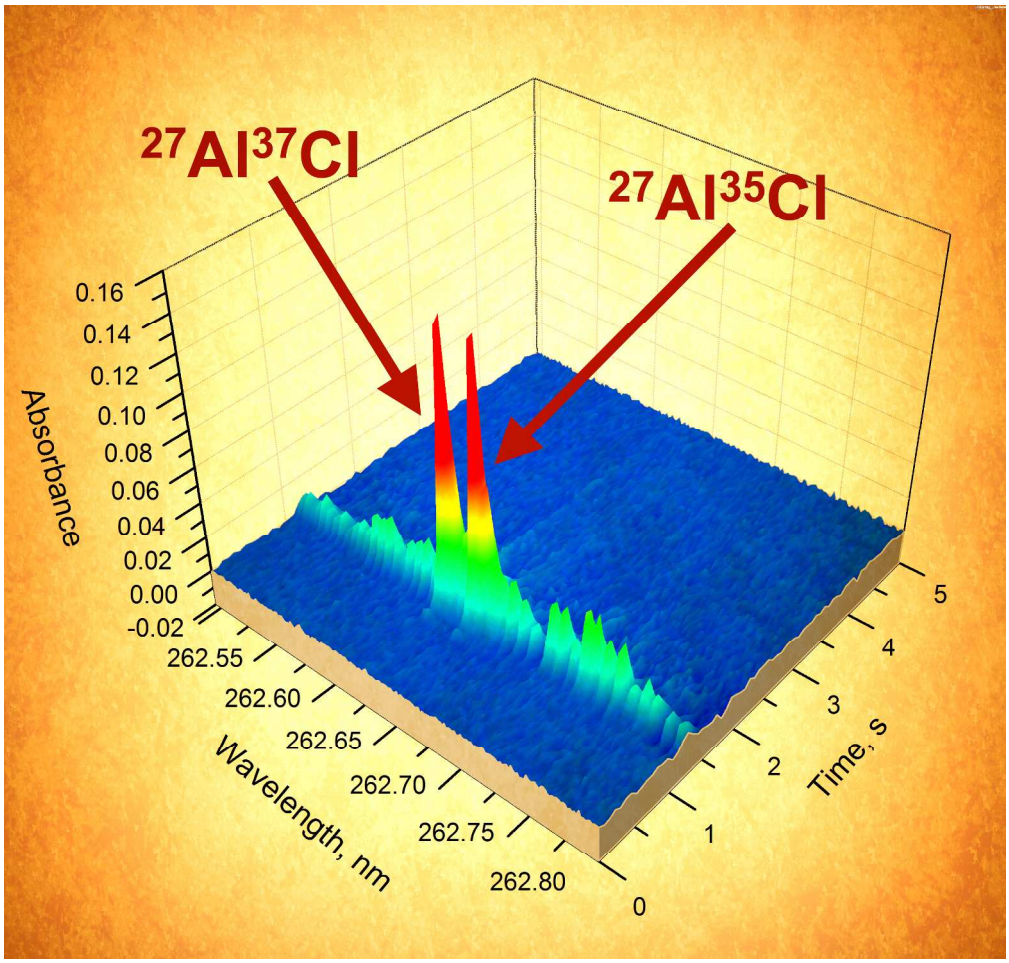

1365x1302mm (72 x 72 DPI)

This article demonstrates the potential of HR CS GFMAS for providing Cl isotopic information and the benefits of using isotope dilution.